Journal of Applied Polymer Science

Processing and properties of phthalic anhydride modified soy protein/glycerol plasticized soy protein composite films

Gaiping Guo,[1] Chen Zhang,[1] Zhongjie Du,[1] Wei Zou,[1] Aimin Xiang,[2] Hangquan Li[1]

[1]Key Laboratory of Carbon Fiber and Functional Polymers, Ministry of Education, Beijing University of Chemical Technology, Beijing 100029, People's Republic of China

[2]School of Material and Mechanical Engineering, Beijing Technology and Business University, Beijing 100048, People's Republic of China

Correspondence to: C. Zhang (E-mail: zhangch@mail.buct.edu.cn)

ABSTRACT: Phthalic anhydride modified soy protein (PAS)/glycerol plasticized soy protein (GPS) composite films were fabricated by using extrusion and compression-molding. Modified with phthalic anhydride, the soy protein lost its thermoplastic ability and was used as a filler to reinforce the GPS matrix. Fourier transform infrared spectra, optical transmittance, scanning electron microscope, mechanical tests, water resistance tests, as well as thermo-gravimetric analysis were carried out to investigate the structure and properties of PAS and the plastic composites. The similar chemical structure of PAS and GPS led to compatibility of the two components resulting in high transparency and enhanced tensile properties of the composites. The water resistance of GPS was also improved by the incorporation of PAS. © 2015 Wiley Periodicals, Inc. J. Appl. Polym. Sci. **2015**, *132*, 42221.

KEYWORDS: biodegradable; biopolymers & renewable polymers; composites

Received 18 December 2014; accepted 10 March 2015
DOI: 10.1002/app.42221

INTRODUCTION

Biopolymers from natural resources have attracted lots of attentions recently for the petroleum crisis and environment pollution.[1–3] Soy protein, a by-product from soybean oil processing, constitutes an abundant renewable plant source.[4] Soy protein isolate (SPI) is a highly refined and purified form of soy protein with a protein content higher than 90% on a moisture-free basis, which is usually used as a starting material for protein-based biodegradable packaging films as well as edible films.[5] When plasticized with small molecules, soy protein behaves like thermoplastic materials with good flexibility, but low mechanical strengths and poor water resistance.[6] In order to overcome such problems, various technical measures were taken, such as blending, filling, etc. The frequently employed blending partners included synthetic polymers, such as polyvinyl alcohol,[7] waterborne polyurethane,[8] poly(butylene succinate),[9] and natural polymers such as cellulose[10] and natural rubber,[11] etc. Incorporation of fillers constitutes another effective way to improve the strength and water resistance of soy protein plastics.[12] The filler can be either organic such as cellulose whiskers,[13] modified starch nanoparticles,[14] or inorganic such as silica,[15] carbon tubes,[16] montmorillonite,[17] calcium carbonate,[18] and nanoboron nitride.[19]

The interaction and compatibility between the components played a key role in reinforcing. The stress of the matrix would be transferred to the filler through interface on the assumption that fine compatibility exist between the filler and matrix. The similarity of the structures of filler and matrix would result in fine compatibility and thus results in the interaction between them. For this reason, some composites such as cellulose whiskers reinforced cellulose films or sponge,[20,21] and starch nanoparticles reinforced thermoplastic starch films[22–24] were developed.

In this study, phthalic anhydride modified soy protein (PAS) was used as a reinforcing filler in glycerol plasticized soy protein (GPS). The interaction and properties of the resulted composites were investigated. It was aimed to pave a simple and economic way to prepare eco-friendly soy protein materials with high performance. It was expected that these composite plastics would find applications in food packaging areas.

EXPERIMENTAL

Material

SPI (moisture ca. 6.5 wt %) was purchased from DuPont-Yunmeng Protein Technology (Yunmeng, China). Other chemicals were obtained from Sinopharm Chemical Reagent (Shanghai, China) and used as received.

Preparation of Phthalic Anhydride Modified Soy Protein

Phthalic anhydride modified soy protein was prepared according to the procedure for N-phthaloylchitosan.[25] Ten g soy protein was dispersed in 200 mL of N,N-dimethylformamide (DMF) and stirred for 2 h. Twenty g phthalic anhydride was added to the resulted solution, and the mixture was stirred at 130°C for 10 h. The mixture after reaction was poured into ice water, centrifuged, and washed with ethanol to obtain a brown N-phthaloyl soy protein powder, which was denoted as PAS.

Preparation of PAS/GPS Composites

Certain amounts of SPI and PAS were mixed and stirred to obtain a homogeneous dispersion. The dispersion was freeze-dried, and was mixed with glycerol at a mass ratio of glycerol/SPI = 1/2. The mixture was first homogenized in a high-speed mixer (HR1704, PHILIPS, Zhuhai, China) for 15 min, and then extruded with a single-screw extruder (PolyDrive with Rheomex R252, ThermoHaake, Germany) with a diameter of 19.1 mm and an aspect ratio of 25 : 1. The screw rotation speed was 40 rpm, and the temperature profile along the extruder barrel was 90°C, 120°C, and 130°C (from feed zone to exit). Subsequently, the extrudate was compression-molded at 140°C for 5 min under a pressure of 20 MPa to obtain PAS/GPS composite plastics. The composite plastics were conditioned in a desiccator with P_2O_5 as desiccant for one week at room temperature before characterization.

Characterization

Fourier transform infrared spectra (FTIR) of the samples were recorded on a Nicolet 5700 FTIR spectrometer (Thermo Electron Corporation, Waltham, MA, USA). The samples were prepared by mixing with fine powder of KBr and pressing. The spectra were obtained at a resolution of 4 cm^{-1} in a range of 4000 to 400 cm^{-1}.

Optical transmittance of the plastics with a thickness of about 0.4 mm was measured with an ultraviolet-visible spectrometer (UV-160A, Shimadzu, Japan) in the wavelength range of 800 to 200 nm.

Scanning electron microscope (VEGA II, TESCAN, S.R.O, Czech Republic) was used to observe the cross-sections of fractured samples. Each sample was frozen using liquid nitrogen, fractured and then vacuum-dried to produce cross-sections. The fractured surfaces (cross-sections) of the plastics were sputtered with gold before observation.

Mechanical properties of the composites were determined using a universal testing machine (Sans, Mts Systems China) in tensile mode according to the ASTM D638 standard at 25°C with a tensile rate of 5 mm/min. Mechanical tensile data were averaged over at least five specimens. The samples were conditioned at 43% RH before testing.

The kinetics of water absorption at room temperature (25°C) was determined for all samples. The specimens with dimensions around 10 × 10 × 0.2 mm^3 were thin enough so that the diffusion was supposed to be unidirectional. The samples were first vacuum-dried overnight at 100°C. After being weighed using a four-digit balance, the samples were conditioned in a desiccator containing K_2CO_3 saturated solution to ensure a RH of 43%. The sample was removed at specific intervals and weighed. The water uptake (WU) was calculated by

$$WU(\%) = \frac{m_t - m_0}{m_0} \times 100 \quad (1)$$

where m_0 and m_t were the weights of the samples before and after a time t of conditioning, respectively.

Thermo-gravimetric analysis (TGA) was performed on a TGA Q5000 thermo-gravimetric analyzer from 25°C to 600°C at a heating rate of 10°C/min under nitrogen atmosphere. The sample mass was about 5–10 mg.

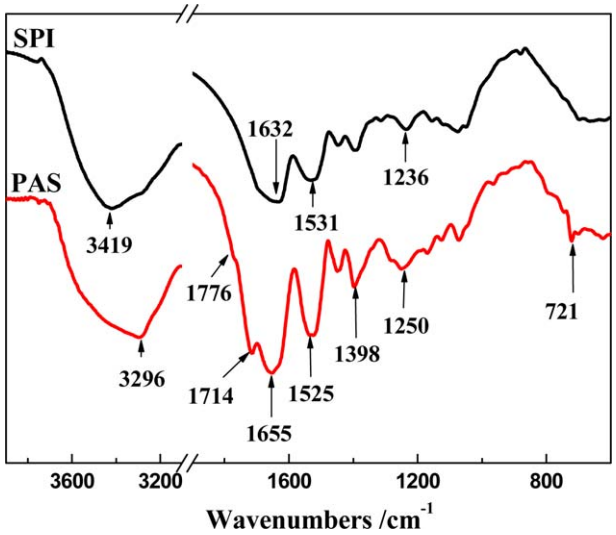

Figure 1. FTIR spectra of SPI and PAS. [Color figure can be viewed in the online issue, which is available at wileyonlinelibrary.com.]

RESULTS AND DISCUSSION

Structural Characterization of PAS

FTIR spectra of SPI and PAS are shown in Figure 1. Typical stretching vibrations of -OH groups (3200–3400 cm^{-1}), amide I (C=O, around 1630 cm^{-1}), amide II (N-H, around 1530), and amide III (C-N, around 1240 cm^{-1}) were observed. The peaks at 1776 and 1714 cm^{-1} indicated C=O imide group existing in N-phthaloyl soy protein. In addition, the peaks at 1398 and 721 cm^{-1} of PAS were assigned to C=C of phthaloyl groups. Scheme 1 was the synthetic route for PAS. Phthalic anhydride could react with $-NH_2$ groups on soy protein, resulting in the decrease of the polar groups.

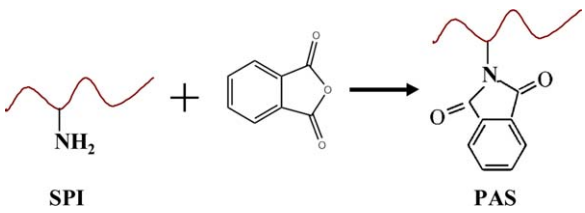

Scheme 1. Synthetic route for N-phthaloyl soy protein. [Color figure can be viewed in the online issue, which is available at wileyonlinelibrary.com.]

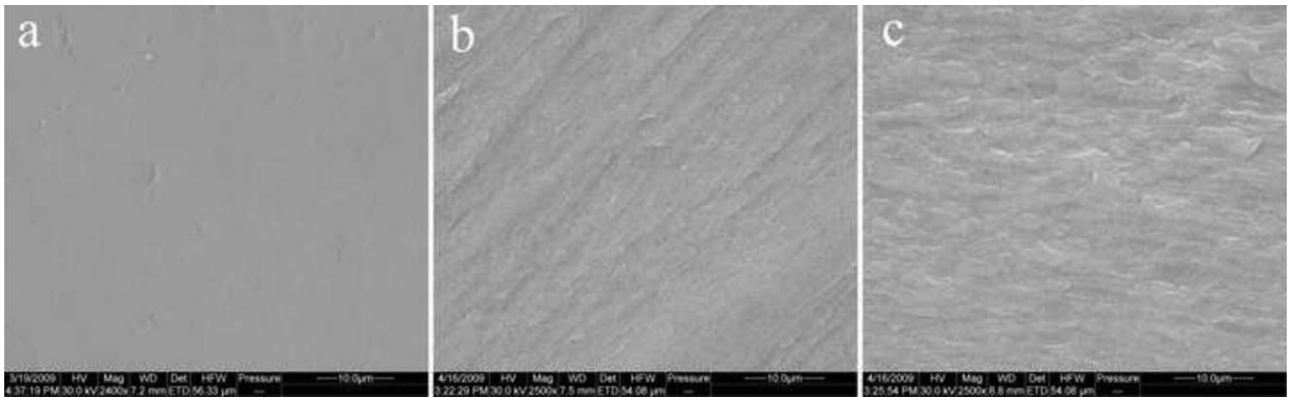

Figure 2. SEM images of thermoplastic soy protein composites with: (a) 0%, (b) 3%, and (c) 9% PAS.

Structure and Interactions of PAS/GPS Composite Plastics

SEM images of PAS/GPS composites with different contents of PAS are shown in Figure 2. Neat GPS exhibited a smooth morphology. With addition of 3% PAS, the morphology became rough, and with 9% PAS, became rougher. In the latter two samples, PAS domains dispersed in GPS matrix homogeneously without obvious aggregation because of the good compatibility between the filler and matrix. The rough folds in morphology were ascribed to the presence of PAS, which possessed poor plasticibility and flowability. When mixed with 50 wt % of glycerol based on neat PAS, the PAS was not able to be hot pressed, indicating the lose of plasticibility after modification. In addition, the C=O groups on PAS may form hydrogen bonds with either plasticizer or the matrix, thus greatly lowered the flowability of the system.

Figure 3 shows the effect of PAS filler on the optical transmittance of the plastics. All the plastics exhibited similar transmittance curves, in which the transmittance decreased with decreasing wavelength. The transmittance descended from its maximum of about 82% at a wavelength of 800 nm to near zero at wavelengths lower than 450 nm. This suggested an excellent anti-ultraviolet property. Owing to the similarity of chemical structures between the filler and matrix again, a good compatibility was achieved. As a result, the inclusion of filler (PAS) affected the transmittance of the matrix slightly.

Mechanical Properties

Figure 4 shows the stress–strain curves of GPS reinforced by various amount of PAS after being conditioned at 43% RH. All the samples indicated a plastic flow after a linear zone without a yielding. However, the flow stress increased with increasing PAS content. The reinforcement of the PAS particles was obvious.

One may also notice that with increasing PAS particle content, the elongation at break decreased. A basic model describing the elongation at break was developed by Nielsen.[26] For the end of perfect adhesion under the assumption that the polymer breaks at the same elongation in the filled system as the unfilled bulk polymer, the elongation at break was given by:

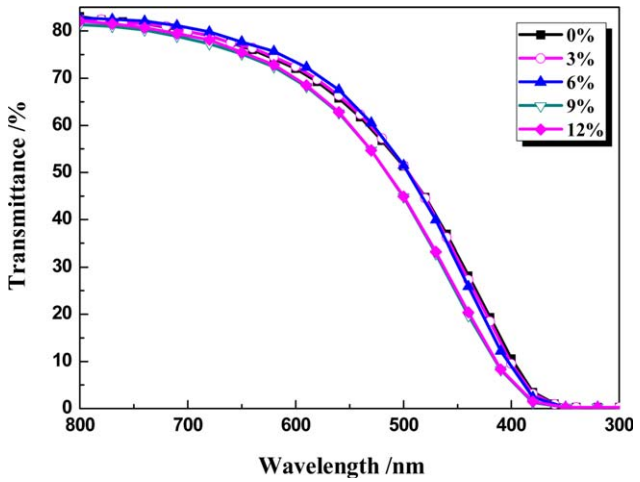

Figure 3. Dependence of Tr on PAS contents for the PAS/GPS plastics. [Color figure can be viewed in the online issue, which is available at wileyonlinelibrary.com.]

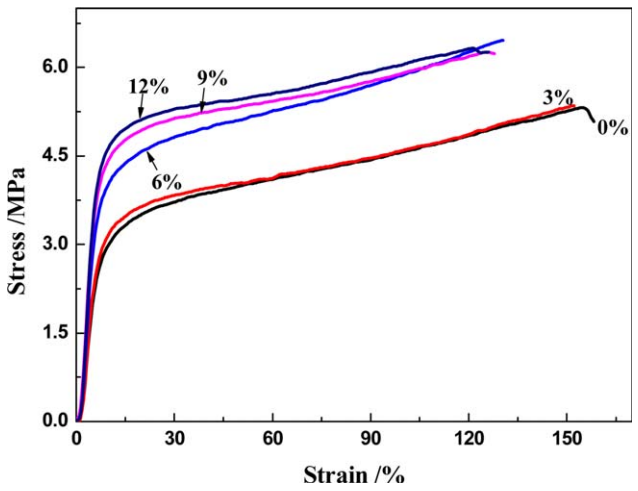

Figure 4. Typical stress–strain curves of PAS/GPS composite plastics. [Color figure can be viewed in the online issue, which is available at wileyonlinelibrary.com.]

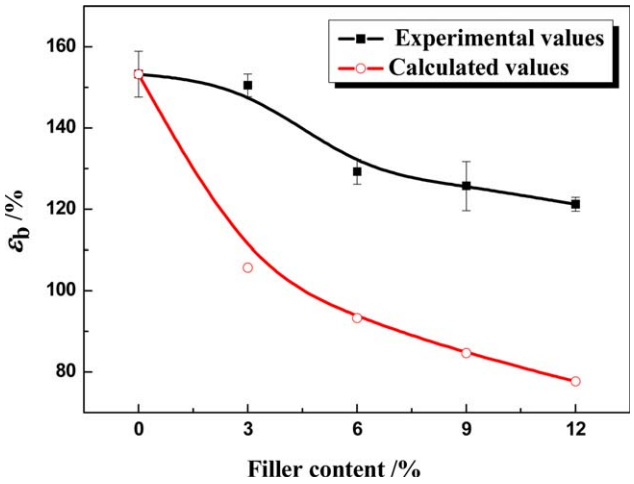

Figure 5. Elongation at break (ε_b) for the composite plastics with different filler contents. [Color figure can be viewed in the online issue, which is available at wileyonlinelibrary.com.]

$$\varepsilon_c = \varepsilon_p(1-\varphi^{1/3}) \quad (2)$$

where ε_c and ε_p are the elongation at break of the composite and the unfilled polymers, respectively. φ was the volume fraction of filler. The values of ε_c were plotted against the filler content and are presented in Figure 5, in which the weight fraction was used instead of volume fraction. It was seen that the experimental values were higher than those calculated using eq. (2). One may conclude that (i) owing to the similar chemical structure of the matrix (GPS) and the filler (PAS), the adhesion was nearly perfect; (ii) the filler was somewhat flexible, not as rigid as inorganic fillers.

With increasing filler content, the tensile strength of the composites increased first, reached the maximum value at 6% PAS, then decreased a little. This behavior may be ascribed to the agglomeration of PAS particles. As aforementioned, at low PAS content (below 6%), PAS was dispersed in GPS matrix homogeneously. However, at higher PAS content (12%), certain content of aggregation might occur, resulting in the decrease of the reinforcement of the filler.

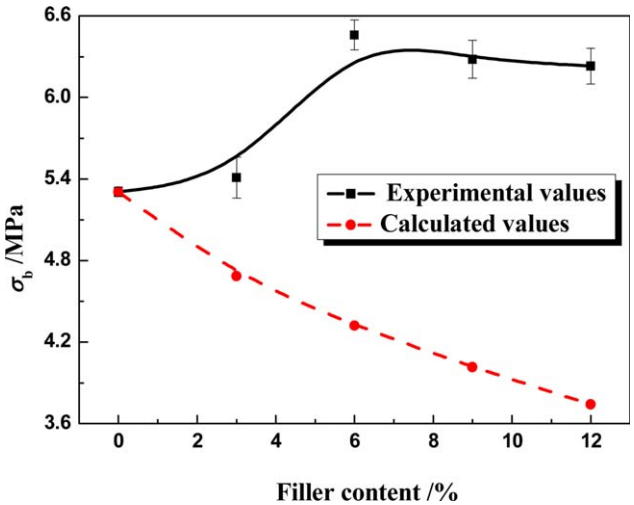

Figure 6. Tensile strength (σ_b) for the composite plastics with different filler content. [Color figure can be viewed in the online issue, which is available at wileyonlinelibrary.com.]

The tensile strength of PAS-filled composites can be predicted by Nicolais–Narkis equation for the end of poor adhesion between the filler and the matrix:[27]

$$\sigma_c = \sigma_m(1-1.21\varphi^{2/3}) \quad (3)$$

where φ, σ_c, and σ_m are volume fraction of the filler, and tensile strengths of the composite and matrix, respectively. By comparing the experimental and calculated ratio of σ_c/σ_m, the adhesion between the filler and the matrix can be described. As shown in Figure 6, the experimental values of σ_c/σ_m were much higher than the ones calculated by eq. (3), indicating a strong interaction between PAS particles and the protein matrix. The good adhesion between PAS and the matrix was also supported by the SEM observation.

Young's modulus of the composite plastics increased linearly with increasing PAS filler. With 12% filler incorporation, Young's modulus increased from 52.9 MPa for GPS to 113 MPa for the composite. Generally speaking, the modulus of the composites was not only influenced by the chemical nature of the matrix and the particles and interaction between them, but also by the interaction among the particles.[28] The modulus of PAS-filled protein can be predicted by taking into account the structure and the deviation from the spherical shape owing to the coagulation of the PAS particles. An attempt had been made to calculate the modulus with Guth reinforcement model for spherical reinforcing particles:[29]

$$E_c = E_m(1+2.5\varphi+14.1\varphi^2) \quad (4)$$

where E_c and E_m were the moduli of the composite and matrix, respectively, and φ is the volume fraction of the filler. The linear term accounts for the reinforcing effect of individual particles, and the second power term corresponds to the contribution of particle pair interactions. For rod-like particles with an aspect ratio f, the modulus of the composite is given by

$$E_c = E_m(1+0.67f\varphi+1.62f^2\varphi^2) \quad (5)$$

By comparing the experimental and calculated values of E_c/E_m, the shape and interaction among the filler particles would be understood. Figure 7 shows the experimental and the calculated moduli according to eqs. (4) and (5). The deviation of E_c/E_m from the calculated value for spherical particles model revealed an existence of the aggregation and interactions between the filler particles. Using f as an adjustable parameter, a better fit was obtained with $f = 6$ for rod-like particles model. Therefore, the occurrence of particle–particle interactions was inferred and the aggregation processes of PAS particles within the polymer matrix led eventually to the cluster formation and deviation from Guth sphere model. The aggregation of PAS would result in the reinforcing effect as rods with aspect ratio of about 6.

Water Resistance

The water resistance of the composites is shown in Figure 8. With increasing filler content, the water uptake decreased

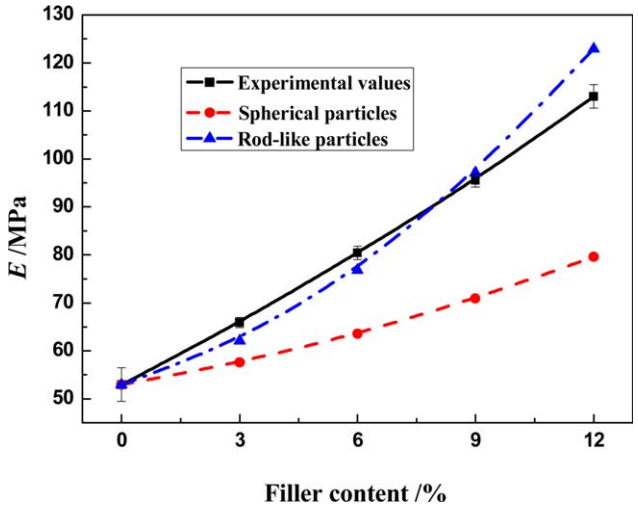

Figure 7. Young's modulus (E) for the composite plastics with different filler contents. [Color figure can be viewed in the online issue, which is available at wileyonlinelibrary.com.]

linearly. PAS would exhibit hydrophobic behavior because of the lowered polar groups, resulting in the improved water resistance. Because of the strong interactions between GPS matrix and PAS filler, the moisture was blocked from the matrix and the overall water uptake was decreased.

Thermal Stability

To evaluate the thermal stability of PAS, TG characterization was carried out on SPI and PAS powders and is shown in Figure 9. Usually, the thermal degradation behavior of SPI consists of two steps: the evaporation of residual moisture (from room temperature to about 120°C) and the degradation of soy protein (above 120°C). PAS exhibited a lower thermal stability than pristine soy protein, which was ascribed to the chemical modification of soy protein macromolecules. The phthaloyl groups on PAS would take off on higher temperatures, leading to the decreased thermal stability of PAS. TG curves of PAS/GPS composite with different filler contents are shown in Figure 10.

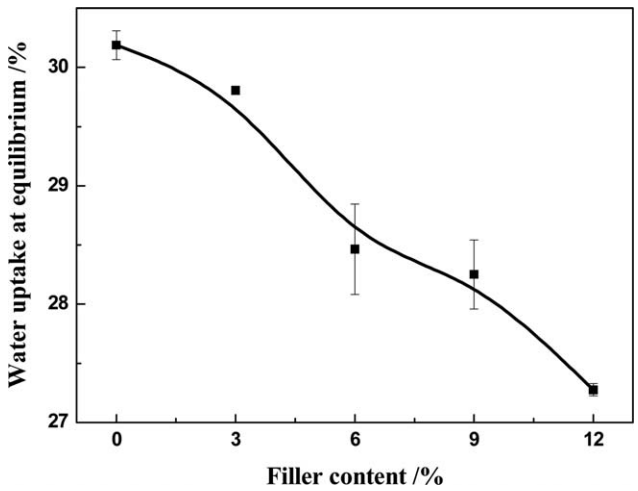

Figure 8. Water resistance properties of composite plastics conditioned at 43% RH.

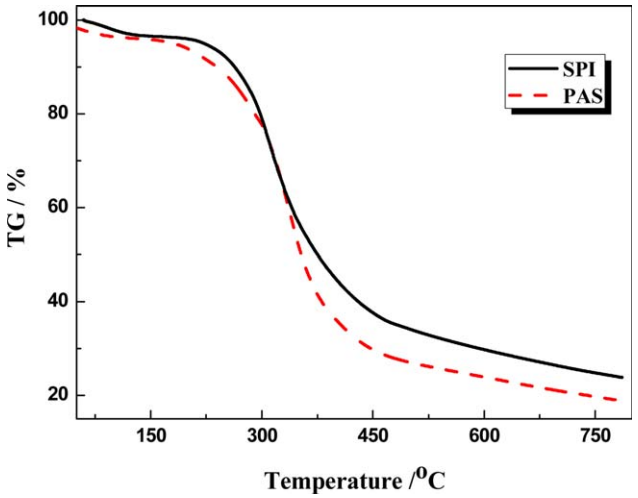

Figure 9. TG curves of SPI and PAS powders. [Color figure can be viewed in the online issue, which is available at wileyonlinelibrary.com.]

All the PAS/GPS composites exhibited three-stage degradation behavior. For temperature below 120°C, the weight loss was ascribed to the residual moisture in the plastics. The evaporation of plasticizers occurred at 120–250°C, and the degradation of soy protein appeared at 250–400°C. All the samples were stable below 160°C except little moisture evaporation. With increasing PAS filler in the composite, the weight loss during the plasticizer evaporation stage decreased, this was obviously for the lowered plasticizer content. However, the weight loss during protein degradation stage for both GPS matrix and PAS filler slightly increased with the increase of PAS filler, which may be resulted by the lower thermo-stability of PAS as indicated above.

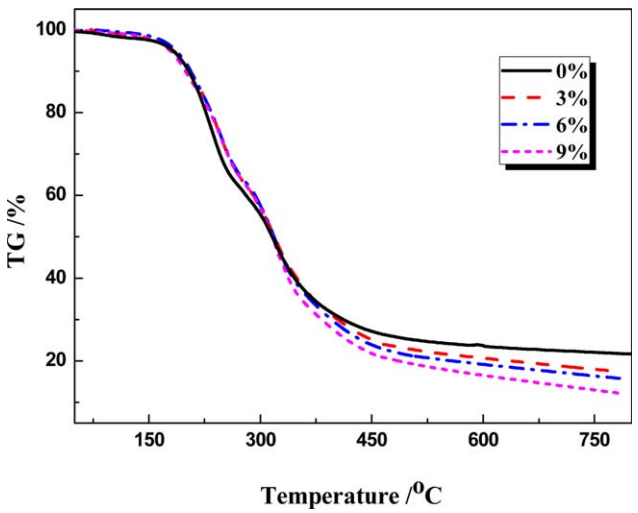

Figure 10. TG curves of PAS/GPS composite plastics with different filler contents. [Color figure can be viewed in the online issue, which is available at wileyonlinelibrary.com.]

CONCLUSIONS

A kind of soy protein composite was prepared from phthalic anhydride modified soy protein (PAS) and glycerol plasticized soy protein (GPS). When soaked with glycerol, PAS was no longer thermoplastic because of the formation of hydrogen bonds and the steric hindrance effect of benzene ring. As a result, PAS behaved as a filler in GPS matrix. Because of the similar chemical structure of the filler and matrix, a good compatibility was observed and the composite kept transparent. PAS provided obvious reinforcing effect on GPS resulting in higher tensile strength and Young's modulus, however, lower elongation at break. The water resistance was also improved because of the incorporation of hydrophobic PAS. PAS exhibited lower thermal stability than pristine soy protein. However, when plasticizer was evaporated, the thermo-stability of PAS was recovered.

REFERENCES

1. Jayaramudu, J.; Reddy, G. S. M.; Varaprasad, K.; Sadiku, E. R.; Sinha Ray, S.; Rajulu, A. V. *Adv. Polym. Technol.* **2013**, *32*, 21349.
2. Liu, D.; Sun, X.; Tian, H.; Maiti, S.; Ma, Z. *Cellulose* **2013**, *20*, 2981.
3. Luo, X.; Mohanty, A. K.; Misra, M. *J. Am. Oil Chem. Soc.* **2012**, *89*, 2057.
4. Kumar, R.; Zhang, L. *Compos. Sci. Technol.* **2009**, *69*, 555.
5. Tian, H.; Xu, G.; Yang, B.; Guo, G. *J. Food Eng.* **2011**, *107*, 21.
6. Tian, H.; Liu, D.; Zhang, L. *J. Appl. Polym. Sci.* **2009**, *111*, 1549.
7. Guo, G.; Zhang, C.; Du, Z.; Zou, W.; Li, H. *J. Polym. Environ.* **2014**, DOI: 10.1007/s10924-014-0682-7.
8. Tian, H.; Wang, Y.; Zhang, L.; Quan, C.; Zhang, X. *Ind. Crop. Prod.* **2010**, *32*, 13.
9. Li, Y.; Zeng, J.; Wang, X.; Yang, K.; Wang, Y. *Biomacromolecules* **2008**, *9*, 3157.
10. Kumar, R.; Anandjiwala, R. D. *J. Appl. Polym. Sci.* **2012**, *124*, 3132.
11. Tian, H.; Zhang, L. *Macromol. Mater. Eng.* **2010**, *295*, 451.
12. Liu, D.; Tian, H. In Natural Polymers; John, M. J., Ed.; Royal Society of Chemistry: London, **2012**; Vol II, Chapter 21.
13. Wang, Y.; Cao, X.; Zhang, L. *Macromol. Biosci.* **2006**, *6*, 524.
14. Tian, H.; Xu, G. *J. Polym. Environ.* **2011**, *19*, 582.
15. Tian, H. *J. Compos. Mater.* **2012**, *46*, 427.
16. Zheng, H.; Ai, F.; Wei, M.; Huang, J.; Chang, P. R. *Macromol. Mater. Eng.* **2007**, *292*, 780.
17. Chen, P.; Zhang, L. *Biomacromolecules* **2006**, *7*, 1700.
18. Liu, D.; Tian, H.; Jia, X.; Zhang, L. *Macromol. Biosci.* **2008**, *8*, 401.
19. Dash, S.; Swain, S. K. *Compos. Sci. Technol.* **2013**, *84*, 39.
20. Wang, Y.; Chen, L. *Carbohydr. Polym.* **2011**, *83*, 1937.
21. Qi, H.; Cai, J.; Zhang, L.; Kuga, S. *Biomacromolecules* **2009**, *10*, 1597.
22. Ma, X.; Chang, P. R.; Yu, *J. Carbohydr. Polym.* **2009**, *75*, 1.
23. LeCorre, D.; Dufresne, A.; Rueff, M.; Khelifi, B.; Bras, J. *J. Appl. Polym. Sci.* **2014**, *131*, 39826.
24. Lan, C.; Yu, L.; Chen, P.; Chen, L.; Zou, W.; Simon, G.; Zhang, X. *Macromol. Mater. Eng.* **2010**, *295*, 1025.
25. Holappa, J.; Nevalainen, T.; Savolainen, J.; Soininen, P.; Elomaa, M.; Safin, R.; Suvanto, S.; Pakkanen, T.; Loftsson, T. M. M.; Järvinen, T. *Macromolecules* **2004**, *37*, 2784.
26. Nielsen, L. E. *J. Appl. Polym. Sci.* **1996**, *10*, 97.
27. Nicolais, L.; Narkis, M. *Polym. Eng. Sci.* **1971**, *11*, 194.
28. Flandin, L.; Hiltner, A.; Baer, E. *Polymer* **2001**, *42*, 827.
29. Guth, E. *J. Appl. Phys.* **1945**, *16*, 20.